Rheology of carboxymethyl cellulose in organic solvents

Anish Gulati[a)] and Carlos G. Lopez[b)]
Materials Science and Engineering Department, The Pennsylvania State University, 80 Pollock Rd, State College, PA 16802, USA

(Dated: 9 February 2026)

Varying the solvent dielectric constant tunes the strength of electrostatic interactions. We report rheological measurements of the semiflexible polyelectrolyte carboxymethyl cellulose in aqueous and non-aqueous media. In non-entangled solutions, the viscosity decreases with decreasing permittivity, consistent with a reduction in effective chain charge. At higher concentrations, solutions become entangled, but the entanglement concentration does not correlate with dielectric constant or effective charge. In several solvents, a further transition occurs: samples change from Newtonian behaviour at low shear with shear thinning at high shear, typical of polyelectrolytes, to shear thinning across the entire shear rate range without a low-shear plateau. We attribute this to enhanced interchain associations at higher concentrations, where more frequent chain contacts and reduced electrostatic repulsion lower the energetic penalty for aggregation.

Keywords: polyelectrolyte, rheology, carboxymethyl cellulose, scattering, organic solvents, viscosity

The conformation of polyelectrolytes in solution is governed by electrostatic interactions between charged groups along the backbone and their screening by counterions and polyions.[1–3] Upon dissolution, counterions partially dissociate from the polymer, leaving the chain with a net charge that generates long range intrachain repulsion which stiffens and swells the chains. The magnitude of the electrostatic interactions is controlled by the dielectric constant of the solvent, since Coulomb energies scale inversely with dielectric permittivity.

In high dielectric media, the energetic penalty for separating oppositely charged species is reduced, favouring counterion dissociation into the bulk solvent.[1,4–6] The resulting increase in effective charge density enhances intrachain repulsion and produces expanded, swollen conformations.[7–9] In contrast, low dielectric solvents promote counterion condensation onto the backbone. This condensation partially neutralizes the chain, lowers the effective charge, and screens electrostatic repulsion, leading to chain contraction.[10,11]

Condensed counterions and fixed charges form ion-pairs that behave as dipoles.[12–14] Interactions between these dipoles introduce short range attractions that can overcome residual electrostatic repulsion and drive intrachain association or collapse of flexible polyelectrolytes,[15,16] even under good solvent conditions.[17] For semiflexible polyelectrolyte carboxymethyl cellulose (CMC), somewhat different behavior has been reported.[18] Small angle scattering measurements showed that lowering the dielectric constant leads to reduced local chain stretching, consistent with conductivity data showing greater counterion condensation. However, no evidence of collapse into globular structures was found.

In this article, we study the solution rheology of CMC in a range of organic solvents spanning an order of magnitude in solvent permittivity. Rheological measurements yield insight into chain dimensions,[3,19] electrostatic screening[20–23] and interchain attractions.[24–26]

CMC is a weak, semiflexible, highly charged polyelectrolyte[27–29] produced industrially by the slurry process via alkalization of cellulose followed by etherification with chloroacetic acid.[30] The degree of substitution is the number of carboxymethyl groups per glucose unit out of a maximum of three. Samples with DS $\lesssim 1$ display partial aggregation due to the presence of unsubstituted cellulose patches along the backbone which act as temporary stickers between chains and can lead to gelation at high concentrations.[26,31–36] Samples with DS $\gtrsim 1$ are molecularly dissolved and no significant aggregation takes place, leading to solution behaviour over the entire concentration range.[37,38] These are known as highly substituted samples. The DS at which cross-over from highly and weakly substituted samples occurs depends on the specific synthesis conditions.

Carboxymethyl cellulose is typically sold and employed as the sodium salt (NaCMC), which is soluble in water but insoluble in most organic solvents except glycerol.[39] Addition of non-solvents such as alcohols or ketones reduces the effective charge of highly substituted CMC and leads to either no change or a small decrease in the specific viscosity.[39–42] For weakly substituted samples, non-solvents promote interchain association, gelation, and ultimately precipitation at high fractions.[43–45] The mechanism of non-solvent induced gelation is not known. Likely, increased counterion condensation with increased non-solvent content reduces the energetic penalty for chains to approach each other, facilitating interchain associations, a phenomenon also observed when the charge density of CMC is reduced by lowering the solution's pH.[36,46,47]

Organic solubility can be enhanced by exchanging alkali counterions for organic ones. Solubility follows Hansen parameters and generally requires polar, hydrogen-bonding solvents, although less protic solvents become effective with organic counterions.[18,48–50] Studies of tetrabutylammonium CMC show that decreasing solvent dielectric constant lowers the effective charge in agreement with Oosawa–Manning condensation theory.[4,5,18,50,51] High dielectric solvents yield

[a)]Institute of Physical Chemistry, RWTH Aachen University, Landoltweg 2, 52074 Aachen, Germany
[b)]Electronic mail: cvg5719@psu.edu.

locally stretched conformations, whereas lower permittivity solvents promote partial folding and weaker electrostatic order, as reflected by less sharp correlation peaks in their scattering function.[18]

MATERIALS AND METHODS

Chemicals: Solvents were purchased from VWR or Sigma Aldrich and used without further purification. The TBACMC used in this study is the same as in earlier works, see refs.[18,52] for details.

Preparation of CMC salts: The NaCMC was converted to its acid form (HCMC) by bringing the pH down to $\simeq 2$ using 0.1 M HCl and then dialysing the resulting solution against DI water to remove the excess ions. The end point of the dialysis was determined by examining the conductivity of the dialysis bath at the point when the conductivity stayed below 2 μS cm^{-1} for at least 4 hours since the last exchange. The resulting solution was frozen using liquid nitrogen and dried under vacuum at a pressure of 0.4 mbar for 72 to 96 hours. The dry HCMC was dissolved in excess TBAOH solution and then subjected to the same dialysis and freeze-drying process to obtain the pure salts.

Sample preparation: The CMC salts were stored in the vacuum freeze dryer for ~ 24 hours before any samples were prepared. The samples were prepared in polypropylene microcentrifuge tubes, previously washed with DI water and dried at 60 °C. All the sample components were added by weight using a balance with a least count of 0.1 mg and, therefore, a typical error of ± 0.05 mg. The samples for rheology measurements with concentrations below 0.02 M were prepared by dilution instead of direct addition of the components.

Rheology: Rheological measurements were carried out on a Kinexus-pro rheometer using cone-plate geometries of diameter 40 mm or 60 mm and angles of 1° and 2°. The temperature was set to 25 °C using a Peltier system. A solvent trap was used to reduce evaporation.

Rolling Ball Viscosimetry: Samples with very low viscosity were measured on a Lovis 2000M microviscometer from Anton Paar. This instrument prevents evaporation during the measurement because of the closed capillary block setup. The rotating capillary block consists of a capillary with a steel ball and measures the time taken by the ball to travel a certain distance at a given angle and reports the dynamic viscosity for a given solution density. The instrument was calibrated against a N2 viscosity standard. For all measurements, the angles were varied from 20° to 70° at 5° intervals. The shear rates for each measurement were also reported by the viscometer.

Small angle X-ray scattering: SAXS experiments were performed at the BL40B2 beamline of the SPring-8 synchrotron (Hyogo, Japan). The sample-to-detector distance was set to 1 m and the X-ray energy to 12.2 keV. Samples were loaded into 2 mm capillaries and sealed with a glue gun to prevent evaporation. Acquisition times were 20 seconds.

Thermogravimetric analysis: The water content of the freeze-dried TBACMC was determined to be 7 wt% using TGA as described in ref. [**?**]. All the concentrations given here are corrected for water-content. The influence of the water content on the viscosity of the solvent is not taken into account as the amount of water is always under 1 wt% of the solution.

RESULTS AND DATA FITTING

Solubility

The solubility of TBACMC in various solvents was checked by mixing the polymer and solvent at a mass ratio of $\simeq 1\%$ and leaving the mixture on a roller mixer for several days. Three different kinds of behaviour could be observed: clear solution, turbid solution, swollen polymer or non-swollen polymer. As listed in Table III, NaCMC is soluble in water, and is not swollen by any other solvent. By contrast, TBACMC is soluble in a wide range of solvents. In Isopropanol, we observed that TBACMC was soluble in the technical grade of IPA but not the reagent grade of the solvent, presumably due to the 2% water content of the former.

A solubility diagram in terms of the Hansen hydrogen-bonding and polarity parameters (δ_H and δ_D respectively) shows that TBACMC is soluble in polar, protic solvents, in agreement with earlier observations[50,53] for another TBACMC polymer

Rheology

In order to avoid evaporation of the samples during measurements, we used a solvent trap over the cone-plate geometry. For samples with relatively low viscosity, e.g. methanol, a larger 65 mm geometry which did not have a solvent trap was used. Measurements were repeated after 10 minutes. If both measurements agreed, it was concluded that no significant evaporation had taken place. The larger geometry consistently gave viscosity values $\sim 7-10\%$ higher than those obtained using the smaller geometry. For some of the low viscosity measurements at high shear rates, we also observed an increase in shear viscosity with shear rate, which we assign to the onset of Taylor instabilities.

The viscosity of TBACMC in 21 solvents was measured as a function of polymer concentration and shear rate. For most solvents, the samples show a Newtonian plateau at low shear rates ($\dot{\gamma}$) followed by shear thinning at sufficiently high $\dot{\gamma}$. Representative results for this kind of flow curves are shown in Figure 1a,b, which compares the viscosity of TBACMC solutions in ethylene glycol and DMSO. In DMSO the flow curves are largely Newtonian over the entire shear rate range studied except for the highest concentrations. By contrast in ethylene glycol, shear thinning is more easily observed due to the relatively high solvent viscosity ($\eta_s \simeq 16$ mPas). For this solvent, the shear rate dependence of the viscosity can be fitted to the Carreau-Yasuda model:

$$\eta(\dot{\gamma}) = \frac{\eta(0)}{[1+(\tau\dot{\gamma})^b]^{n/b}}$$

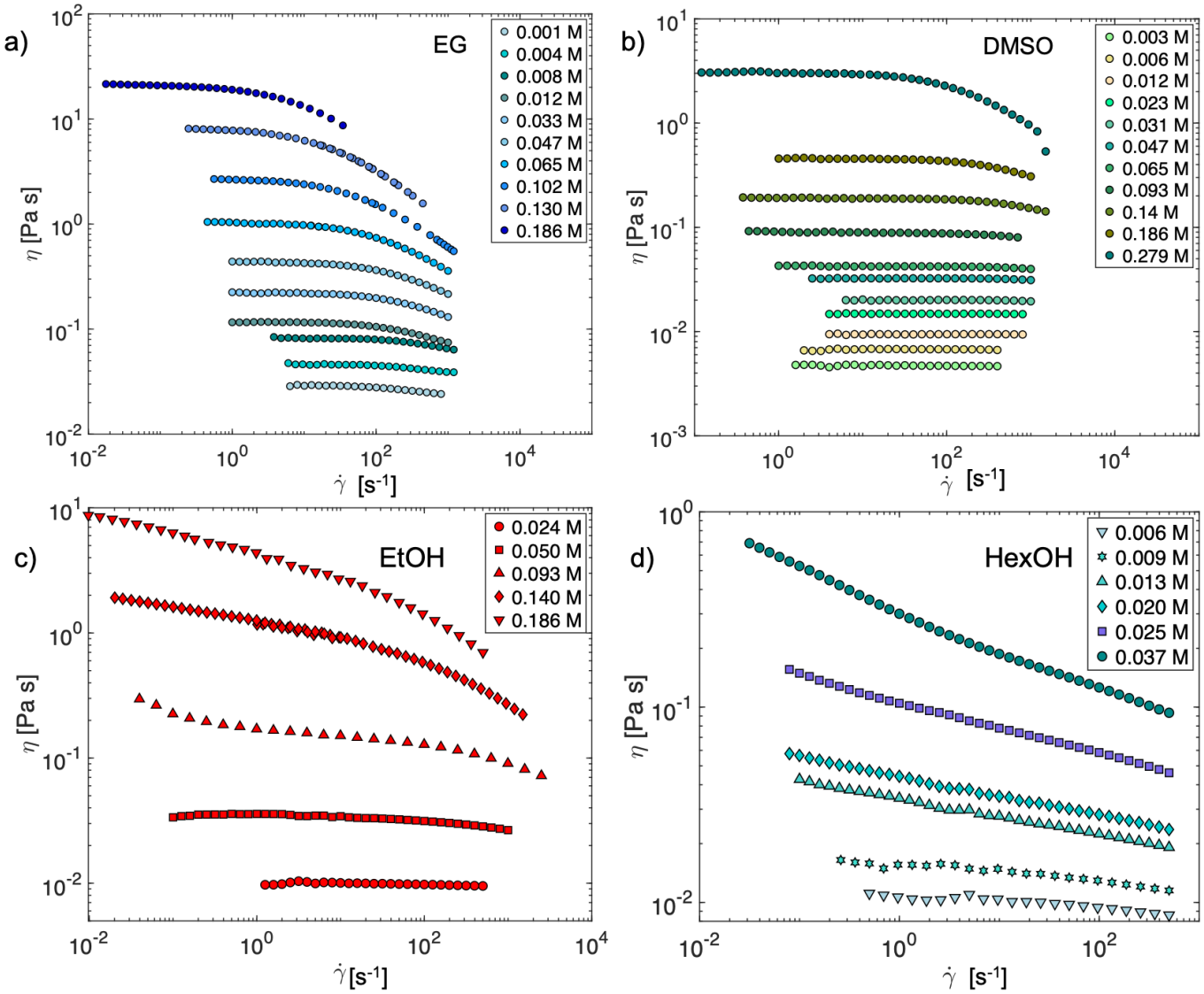

FIG. 1. Viscosity (η) as a function of shear rate ($\dot{\gamma}$) for TBACMC in a) EG, b) DMSO, c) EtOH and d) HexOH. In EG, the curves show a Newtonian behaviour at low $\dot{\gamma}$ followed by a distinct shear thinning at high $\dot{\gamma}$. The curves in DMSO are largely Newtonian over the entire range of measured $\dot{\gamma}$ except at the highest concentrations where shear-thinning behaviour becomes more evident. In EtOH and HexOH, transition from solvophilic to associative behaviour (characterized by the disappearance of the Newtonian plateau at low $\dot{\gamma}$) at high concentrations can be seen.

where $\eta(0)$ is the zero-shear-rate viscosity, τ is the longest relaxation time of the system, n is the flow index and b a fitting parameter that sets the sharpness of the Newtonian to power-law transition. The fitted values for these parameters are listed in the supporting information.

For some solvents, samples do not display a Newtonian plateau beyond a critical concentration, and the apparent viscosity shows an increase with decreasing shear rate over the entire measured $\dot{\gamma}$ range. An example of this kind of behaviour, which was observed for all the linear alcohols studied (methanol to 1-hexanol) is shown in Figure 1c and 1d. The existence of the plateau is confirmed by the presence of a region of shear rate independent viscosity extending for around one order of magnitude with a torque higher than the minimum acceptable torque of the rheometer, determined to be $\simeq 4\times10^{-6}$ N m.

I. DISCUSSION

The specific viscosities of the solutions were calculated as $\eta_{sp} = (\eta - \eta_s)/\eta_s$, where η is the viscosity of the solution in the Newtonian region and η_s is the viscosity of the solvent, listed in Table III. Figure 2 compares the concentration dependence of the specific viscosities of NaCMC and TBACMC in aqueous solutions without added salts. The results are seen to agree well over the entire concentration range studied. This same behaviour was observed for different salts of polystyrene sulfonate, where specific viscosities were found to be independent of the counterion type as long as the polyelectrolyte

volume fraction was not high.[49] The data in figure 2 were fitted to a cross-over function:[22,54,55]

$$\eta_{sp}(c) = \left(\frac{c}{c^*}\right)^{\alpha}\left[1+\left(\frac{c}{c_e}\right)^{\beta-\alpha}\right] \quad (1)$$

where c^* is the overlap concentration, c_e is the entanglement concentration and α and β are the exponents in the semidilute unentangled and semidilute entangled regimes respectively.

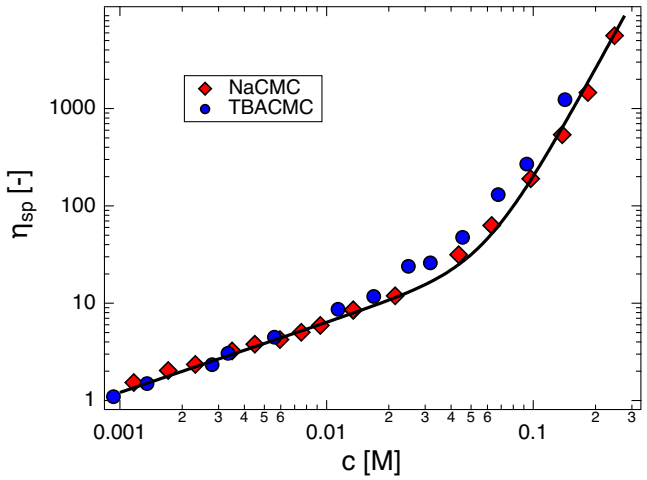

FIG. 2. Specific viscosities of NaCMC and TBACMC as a function of concentration in DI water without added salts. Line is Eq. 1.

For solvents where the samples do not display a Newtonian plateau over a sufficiently wide concentration range to fit Eq. 1, we fit a power-law around the $\eta_{sp} \simeq 1$ region and identify c^* from the point where the fit crosses $\eta_{sp} = 1$. The viscosity of TBACMC in 0.1 M TBABr was measured in ten solvents and the overlap concentration was determined using the $\eta_{sp}(c^*) = 1$ criterion. The resulting values of c^* and c_e in solvents without added salt and for c^* in 0.1 M TBABr are listed in Table I.

Solvents typically contain residual salts which modify the screening length of the media. Hence, polyelectrolyte solutions can rarely be considered as 'salt-free'. Here we use the solvent conductivity and viscosity, listed in the appendix, to estimate the residual salt content of the various solvents used. Assuming the residual salt ions have similar mobilities to sodium chloride $\Lambda_{Cl^-} = 76.3$ Scm^{2}mol$^-$1 and $\Lambda_{Na} = 50.1$ Scm^{2}mol$^-$1, the residual salt can be estimated as:

$$c_{res}[M] \simeq \frac{\sigma_s \eta_s}{126.4 \times 0.89} \quad (2)$$

where σ_s and η_s are the solvent's conductivity in S/cm and viscosity in mPas respectively. Eq. 2 assumes that the mobility of the ions is inversely proportional to the solvent viscosity.

Of the various solvents considered, only 1,3-propanediol has a residual salt concentration approaching the millimolar range, with others typically having $c_{res} \simeq$ 1-40 μM, which influences the viscosity only modestly over the concentration range studied.

Solvent	c_{res} [μM]	c^* [mM]	c^*_{SF} [mM]	c_e [mM]	c^*_{ES} [mM]
Dimethylsulfoxide	9.6	1.76	1.67	118.3	10.45
Ethylene Glycol	12.0	1.28	1.16	58.2	7.32
Water	15.9	0.87	0.79	52.7	4.95
Dimethylformamide	8.4	2.79	2.70	21.9	
Propylene Glycol	2.1	2.53	2.51		6.82
1.2-Butanediol	8.9	3.37	3.20	59.8	7.53
1,4-Butanediol	19.6	2.50	2.26		6.21
Dipropylene Glycol	–	3.77	3.77	68.1	6.76
Diethylene Glycol	30.2	2.75	2.38		
Ethanol	1.4	3.04	3.01	49.3	5.65
Triethylene Glycol	14.3	4.66	4.41		
Propanol	1.7	2.73	2.70		
1-Pentanol	0.9	4.63	4.60		
Isoamyl Alcohol	0.4	4.86	4.85		
1-Butanol	4.1	4.50	4.40		
Methanol	4.0	2.45	2.40	49.3	
1,3-Propanediol	402.4	2.14	0.52	63.5	7.08
Tripropylene Glycol	11.6	7.76	7.35		9.01
1-Hexanol	0.3	5.09	5.08		
1,2-Pentanediol	42.2	7.71	6.76		

TABLE I. Overlap concentrations under no-added salt and excess salt conditions and entanglement concentration under no-added salt conditions for TBACMC in different solvents. The overlap concentrations in solvents without added salt and in 0.1 M TBABr were determined from the point at which $\eta_{sp} = 1$.[19]

A. Overlap concentration

According to the scaling model, the effect of residual salt is to increase the overlap concentration by a factor of: $\left[1+\frac{2c_S}{fc}\right]^{1.5}$. Following our earlier work, we estimate the fraction of monomers with a dissociated counterion as: $f = 0.5\varepsilon/78$. With this, and the estimate of c_{res} from Eq. 2, we can estimate c^*_{SF} in the various solvents measured. For most solvents, the correction in c^* due to residual salt is relatively small (< 15%). The exceptions are 1,2 pentanediol ($c^*_{SF}/c^* \simeq 1.2$) and 1,3-propanediol ($c^*_{SF}/c^* \simeq 2.6$).

The overlap concentration of TBACMC is plotted as a function of solvent dielectric constant in Fig. 3 for solvents without added salt and in 0.1 M TBABr. In the absence of added salt, the data follow a power law, $c^* \propto \varepsilon^{-1}$. This dependence is weaker than the scaling $c^* \sim \varepsilon^{-2}$ reported for several flexible polyelectrolytes.[3,11,49,56] In excess salt, a weaker scaling, $c^* \propto \varepsilon^{-0.25}$, is observed. The decrease in c^* with increasing dielectric constant is qualitatively expected because higher solvent permittivity promotes counterion dissociation,[18] which increases electrostatic chain expansion. We next compare these results with predictions from scaling theory and double screening theory.

1. Solutions without added salt

Scaling theory describes dilute, salt-free polyelectrolyte chains as strings of electrostatic blobs of size ξ_{el}, each containing $g_{\xi,el}$ monomers. For $c < c^*$, the end-to-end distance

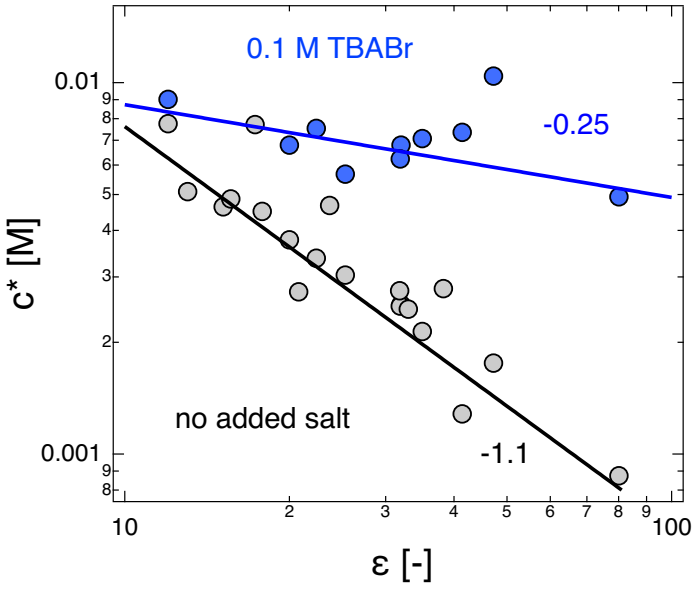

FIG. 3. Overlap concentration of TBACMC in solvents without added salt (grey circles) and in 0.1 M TBABr solutions (blue circles). Data without added salt have been corrected for the residual salt content, see text. Lines are best fit power-laws with the exponent indicated on the graph. The fit to the excess salt data excludes the DMSO datum. The values of c^* are determined from the point at which $\eta_{sp} = 1$.[19]

is:

$$R \simeq \frac{bN}{B} \tag{3}$$

where b is the monomer size, N the degree of polymerisation, and B the stretching parameter, which quantifies chain folding within an electrostatic blob ($B = g_{\xi,el} b/\xi_{el}$).

For a theta solvent, or when the thermal blob size exceeds the electrostatic blob size, the stretching parameter scales as:

$$B = b^{2/3} l_K^{-1/3} (l_B f^2)^{-1/3} \tag{4}$$

where l_K is the intrinsic Kuhn length, f the fraction of dissociated monomers, and l_B the Bjerrum length. According to Oosawa–Manning theory, $f \propto l_B^{-1}$, so Eq. 4 reduces to $B \propto (l_K/l_B)^{-1/3}$.

Muthukumar's theory gives a similar result:[7,57]

$$R_g \simeq 0.2 (f^2 l_K^{-2} l_B)^{1/3} Nb \tag{5}$$

Again if we use the $f \propto l_B^{-1}$ relationship which we experimentally determined for TBACMC in an earlier study, Eq. 5 expects $R_g \propto (l_K/l_B)^{-1/3}$, in agreement with the scaling model.

The overlap concentration follows from the space-filling condition, $c^* \simeq N/R^3$, and according to the scaling theory is:

$$c^* \simeq \frac{B^3}{b^3 N^2} \tag{6}$$

The predicted N^{-2} scaling for salt-free polyelectrolytes, including NaCMC, has been confirmed experimentally.[2,28,58,59]

Combining Eqs. 4 and 6 with the Oosawa–Manning relation gives:

$$c^* \propto (\varepsilon l_K)^{-1} \tag{7}$$

The double screening theory of Muthukumar[57,60]**?** leads to the same result if $f \propto l_B^{-1}$ is assumed.[61]

Direct comparison between Eq. 7 and the experimental data in Fig. 3 is limited because the solvent dependence of the Kuhn length of CMC is unknown. For many aliphatic polymers the Kuhn length is weakly dependent on solvent and temperature,[62–65] whereas several cellulose derivatives show strong solvent-type[66–72] and temperature[73] dependences. A further limitation is that the derivation of Eq. 4 assumes that the chain is flexible within an electrostatic blob, i.e., $\xi_{el} > l_K$. For highly charged polyelectrolytes, ξ_{el} is expected to be comparable to the Bjerrum length. In water, $l_B \simeq 0.7$ nm whereas the Kuhn length of CMC is $\simeq 10$ nm, so this condition is not satisfied and Eq. 4 may not apply. At low ε in Fig. 3, $l_B \simeq 4$ nm. Because the Kuhn length in these solvents is unknown, it is not possible to determine whether $l_K < l_B$.

Comparison with other systems

The dependence of c^* on solvent dielectric constant has been investigated for three flexible polyelectrolytes: two poly(ionic liquid)s[11,56] (see 3 for a discussion of these data) and polystyrene sulfonate.[49] The poly(ionic liquid)s follow $c^* \propto \varepsilon^{-2}$, while PSS shows $c^* \propto \varepsilon^{-1.7}$. Both exponents are larger in magnitude than those observed for CMC.

Two explanations may account for this difference. First, the data of Dayan et al.[66] and Kamide et al.[67,74] show a positive correlation between the Kuhn length of several cellulose derivatives and solvent permittivity. If a similar dependence applies to CMC, and since c^* is expected to scale linearly with the Kuhn length, the intrinsic ε dependence at constant l_K would be stronger than the observed -1 exponent. In this case, variations in l_K with solvent would partially mask the dielectric scaling, leading to an apparently weaker dependence compared with flexible systems such as PSS and poly(ionic liquid)s. Second, PSS and the poly(ionic liquid)s are flexible polyelectrolytes with $l_K \lesssim \xi_{el}$, whereas CMC is semiflexible with $l_K > \xi_{el}$. The two systems therefore lie in different conformational regimes, and different scaling relations are expected to apply.

The data of Dou and Colby[21] provide a related comparison. For quaternised PV2P in ethylene glycol at low degrees of quaternisation, they reported $c^* \propto f^{-1.3}$, which deviates from the scaling predictions for theta or good solvents.[3] In that system the Bjerrum length is constant, so changes in c^* reflect variations in the effective charge fraction alone. By contrast, in the solvent-dependent studies discussed above, both the charge fraction and the strength of electrostatic interactions vary simultaneously. The results of Dou and Colby therefore indicate that the scaling model does not fully capture the dependence of chain size on effective charge fraction, an effect that cannot be isolated as clearly in the other experiments.

Comparison with scattering data

Not knowing the Kuhn length of CMC in organic solvents makes testing the scaling ideas from c^* difficult, but we can

TABLE II. Comparison of stretching parameter and dimensionless ratio $c^*N^2b^3/B^3$ for three polymers. Data are from this work and [11,17, 18,49,75]. Only data for solvents showing $\xi \propto c^{-1/3}$ included. [a] corrected for residual salt in the solvent, see ref. [3,11] [b] result for CsPSS, taken from ref. [76]

		TBACMC ($N \simeq 910$)			TBAPSS	($N \simeq 1354$)		PC4TFSI	($N \simeq 2470$)	
Solvent	l_B [nm]	c^* [mM]	B [-]	$\frac{b^3}{c^*B^3N^2}$ [-]	c^* [mM]	B [-]	$\frac{b^3}{c^*B^3N^2}$ [-]	c^* [mM]	B [-]	$\frac{b^3}{c^*B^3N^2}$ [-]
N-methyl-methyl acetamide	0.30							0.043[a]	1.56	1.5328
N-methylformamide	0.30									
Water	0.71	0.9	1	0.01822	0.6	1.58	0.3839			
Propylene carbonate	0.86							0.77	1.71	0.1127
Dimethyl sulfoxide	1.20	1.9	1.26	0.01726	0.53	1.60	0.4472	1	1.64	0.0766
3-methylsulfolane	1.90							3.4	3.36	0.1937
N,N-dimethylformamide	1.50	3	1.7	0.02685				1.7	1.95	0.0757
Ethylene glycol	1.46	1.4	1.3	0.02573	1.7	2.40	0.4713			
Acetonitrile	1.46				2.9	1.92	0.1411			
Methanol	1.73	3	1.4	0.01500	2.2	1.69	0.1274			
Ethanol	1.98	3.3	2.5	0.07764	3.8	2.30	0.1864			

overcome this by considering ratios of experimental observables where the Kuhn segment does not appear. The scaling theory predicts the ratio $\frac{b^3}{c^*B^3N^2}$ to be a constant and of order unity, independent of the polymer's Kuhn length.

Table II reports the ratios $\frac{B^3}{c^*b^3N^2}$ for three polyelectrolytes, TBAPSS, poly(1-butyl-3-vinylimidazolium bis(trifluoromethanesulfonyl)imide) (PC4TFSI), and TBACMC. The stretching parameter B is obtained from small-angle scattering experiments, where the position of the correlation peak is measured as a function of concentration, see [17,18,75]. The overlap concentration is evaluated viscosimetrically using the same procedure as in the present work. Equation 6 predicts that this ratio should be independent of solvent and of order unity, independent of solvent and polymer. The double-screening theory likewise expects this quantity to be independent of both solvent and polymer chemistry.

Neither expectation is fully satisfied by the data. The deviation from unity is not unexpected, since the chain dimensions at the overlap concentration are significantly smaller than those at infinite dilution, where Eq. 3 applies. The variation of $\frac{b^3}{c^*B^3N^2}$ for a given polymer across different solvents is more difficult to rationalise and points to a limitation of the scaling prediction. We note, however, that because $B^3 \propto \xi^6$, experimental uncertainties in the determination of the correlation length are strongly amplified in the calculation of $\frac{b^3}{c^*B^3N^2}$. Finally, the light-scattering estimate $N = 2470$ for PC4TFSI is likely an underestimate, since the refractive index increment was not determined under conditions of constant chemical equilibrium.[11]

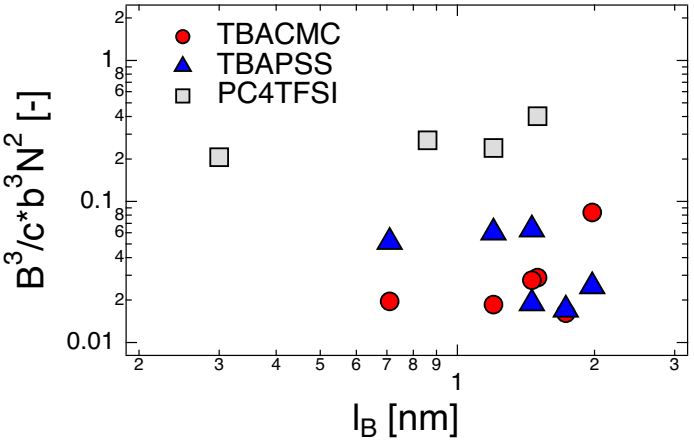

FIG. 4. Dimensionless ratio $B^3/(c^*b^3N^2)$ as a function of solvent Bjerrum length for three polyelectrolytes. Data are from this work and [11,17,18,49,52,75]. Degree of polymerisation at 910 for TBACMC, 1370 for TBAPSS and 2470 for PC4TFSI.

2. *Excess salt solutions*

The overlap concentration data in salt-free solutions and in the presence of 0.1 M TBABr converge at $\varepsilon \simeq 10$, which presumably corresponds to the dimensions of the CMC chain in the absence of electrostatic stiffening or swelling. Notably, this value of ε coincides with the solubility limit of TBACMC. Solvents with lower dielectric constants do not dissolve TBACMC.

In the excess-salt limit, $fc/(2c_S) \ll 1$, scaling theory predicts the size of a chain in dilute solution as

$$R \simeq b^{2/5}B^{-2/5}N^{3/5}f^{1/5}(2c_S)^{-1/5}, \tag{8}$$

where the factor $B^{-2/5}$ accounts for the reduction of the effective contour length as the electrostatic blob size increases, and the term $(f/c_S)^{1/5}$ reflects the role of electrostatic repulsion in stiffening and swelling the chain. Assuming again that $f \propto l_B^{-1}$, Eq. 8 predicts $R \propto \varepsilon^{1/3}$ and $c^* \propto \varepsilon^{-1}$, identical to the scaling obtained for salt-free solutions.[77] This prediction is in strong disagreement with the experimentally observed trend.

It is important to note that the scaling $c^* \propto \varepsilon^{-1}$ arises from two distinct contributions. The first is the shortening of the effective contour length, captured by the $B^{-2/5}$ term in Eq. 8, and the second is electrostatic stiffening and swelling, described by $(f/c_S)^{1/5}$. Since $B^{-2/5} \propto \varepsilon^{0.13}$ and $(f/c_S)^{1/5} \propto$

$\varepsilon^{0.2}$, each contribution alone predicts a dependence of c^* on solvent permittivity that is stronger than that observed experimentally in Fig. 3.

As in the salt-free case, a direct test of Eq. 8 is hindered by the lack of information on how the Kuhn length varies with solvent. Experimental trends reported for other cellulose derivatives indicate that l_K *increases* with increasing dielectric constant, making it unlikely that a solvent-dependent Kuhn length can reconcile the discrepancy between the experimental data and the scaling prediction.

In the large-N limit, the double-screening theory[60,78] gives the same scaling form for the chain size as Flory's theory:[79]

$$R_g = l_K^{2/5}\left[w_0 + w_{el}\right]^{1/5} N^{0.6} \tag{9}$$

where w_0 is the intrinsic (no-electrostatic) excluded volume and w_{el} is the electrostatic excluded volume, which scales as $w_{el} \propto f^2 l_B^{-1}/c_S$. Substituting the $f \propto l_B^{-1}$ relationship found in ref. [18], Eq. 9 predicts a crossover from $R_g \propto l_B^0$ when $w_0 \gg w_{el}$ to $R_g \propto l_B^{-0.2}$ when $w_0 \ll w_{el}$.

The overlap concentration follows from Eq. 9 using the space-filling condition $c^* \simeq N/(\sqrt{6}R_g)^3$. Equation 9 therefore predicts a crossover from $c^* \propto l_B^0$ when the intrinsic (non-electrostatic) excluded volume dominates to $c^* \propto l_B^{-0.6}$ when the electrostatic excluded volume dominates. In practice, since both w_0 and l_K (and hence w_{el}, which depends on l_K) may themselves depend on solvent dielectric constant, a direct test of Eq. 9 against the present data is not straightforward.

B. Semidilute unentangled solutions

Figure 5 plots the power-law exponent of the specific viscosity as a function of concentration near the overlap point as a function of solvent dielectric constant. At high ε, the exponent approaches a value of $\simeq 0.7$, consistent with earlier reports.[37,54,80] This value is larger than the Fuoss-law prediction of $1/2$, which is observed for flexible polyelectrolytes such as NaPSS[76,81,82] and other systems.[9,21] A discussion of this discrepancy can be found in refs. [8,39,83]. As the dielectric constant decreases, the apparent η_{sp}–c exponent increases and reaches a value of $\simeq 1.3$, which matches the prediction for neutral polymers in good solvents.[83,84]

The scaling theory predicts:[1,85]

$$\eta_{sp} \propto c^{\nu/(3\nu-1)}, \tag{10}$$

where ν relates the number of monomers in a correlation blob, g_ξ, to its size as $\xi \propto g_\xi^\nu$. For polyelectrolyte solutions, the theory predicts $\eta_{sp} \propto c^{1/2}$ when the correlation length satisfies $\xi \gtrsim \xi_{el}$, and $\eta_{sp} \propto c^{1.3}$ when $\xi_{el} \lesssim \xi \lesssim \xi_T$, where ξ_T is the thermal blob size.[83] The data in Fig. 5 may therefore be interpreted as reflecting a crossover from the regime $\xi \gtrsim \xi_{el}$ at high dielectric constant to $\xi_{el} \lesssim \xi \lesssim \xi_T$ at low ε.

The scaling theory predicts the viscosity of non-entangled polyelectrolyte solutions to be

$$\eta_{sp} = N(cb^3)^{1/2} B^{-1.5}\left[1 + \frac{2c_S}{fc}\right]^{-3/4}. \tag{11}$$

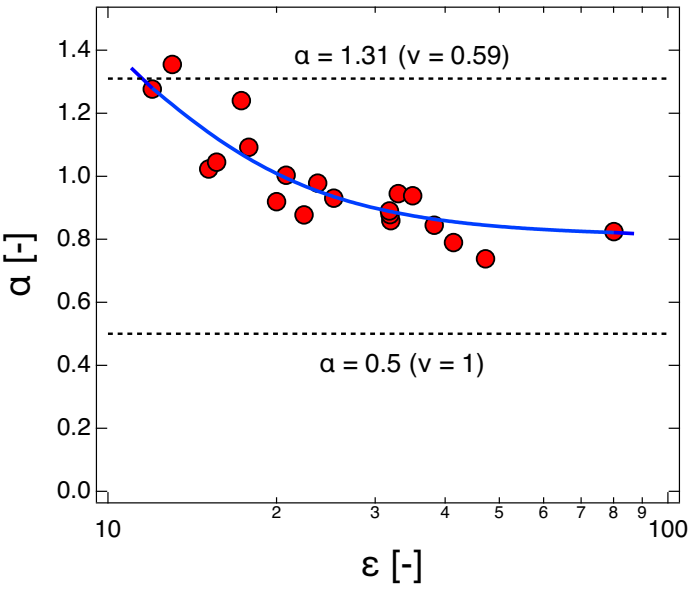

FIG. 5. Non-entangled viscosity exponent (α) close to the overlap point as a function of solvent dielectric constant. Blue line is a guide to the eye and dashed lines are scaling predictions for salt-free polyelectrolyte and neutral polymer in good solvent cases.

Figure 6 plots the specific viscosity at $c = 0.009$ M in solutions without added salt as a function of solvent dielectric constant. The specific viscosity values are normalised by $[1 + 2c_{S,res}/(fc)]^{-0.75}$ to correct for the effect of residual salt in the solvent. This correction is only significant for 1,3-propanediol, where $[1 + 2c_{S,res}/(fc)]^{0.75} \simeq 1.28$. For the remaining solvents, the residual salt correction does not exceed a few percent.

At low solvent permittivities, electrostatic interactions are expected to have a minor effect on chain conformation and dynamics, and the solutions lie above c_D, which takes a value of $\simeq 0.01$ M for $\varepsilon \simeq 10$, as discussed above. As the dielectric constant increases and counterion dissociation becomes more pronounced, c_D increases. One estimate places c_D for NaCMC in water at 0.016 M,[83,86] while other reports expect somewhat larger values.[28,54]

The data follow a power law $\eta_{sp} \sim \varepsilon^{0.78}$, which implies $B \propto \varepsilon^{0.26}$. As in the preceding discussion, direct comparison with theoretical predictions is limited by the unknown dependence of the Kuhn length on solvent type. Assuming l_K to be independent of solvent, the scaling theory predicts $B \propto \varepsilon^{0.29}$ for good solvents and $B \propto \varepsilon^{0.33}$ for theta solvents.

At a higher concentration of 0.035 M, still in the non-entangled region, the viscosity of TBACMC is found to be independent of dielectric constant in the 20-50 range. This presumably occurs because at this concentration the correlation length has decreased to a point where $\xi \lesssim \xi_{el}$ and the solutions are in the $c > c_D$ regime. The exception to this trend is water, which has a higher specific viscosity. This may be a particularity of water or it may signal that c_D is higher than 0.035 M, which is consistent with the viscosity vs. added salt data from ref. [54].

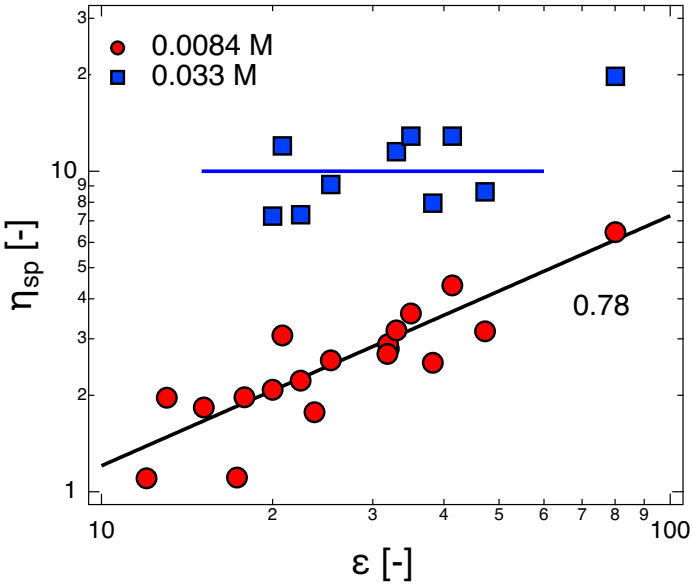

FIG. 6. Specific viscosity of TBACMC as a function of solvent permittivity. The black line is a best-fit power-law with exponent of 0.78. The red circles are for $c = 0.009$ M and the blue squares for $c = 0.035$ M.

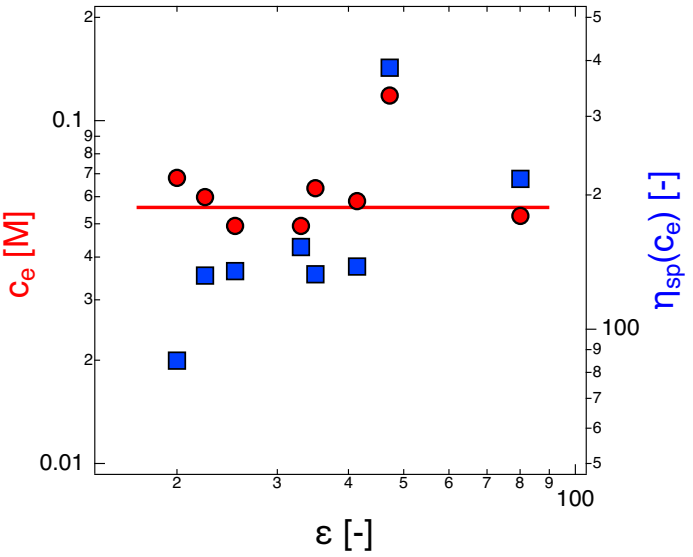

FIG. 7. Entanglement concentration and viscosity at the entanglement point as a function of solvent dielectric constant.

C. Entanglement concentration

The interpretation of entanglement behaviour in polyelectrolyte solutions is complicated by the fact that, for flexible chains with $N \lesssim 4000$, the entanglement concentration often coincides with the onset of the concentrated regime and with a transition to a concentration-dependent monomeric friction coefficient. As a result, the identification of a well-defined entanglement point becomes ambiguous. This issue is discussed in detail in refs. [28,76,83,87–90]. Semiflexible polyelectrolytes are interesting because entanglement occurs at much lower concentrations, where local friction is essentially concentration independent and c_D is expected to occur at lower values than for flexible systems.

Fig. 7 plots the entanglement concentration as a function of solvent dielectric constant. No dependence of c_e on the relative permittivity is observed. The specific viscosity at the entanglement point, $\eta_{sp}(c_e)$ appears to show a weak positive correlation with solvent dielectric constant. The $c_e \propto \varepsilon^0$ dependence can be explained by noting that for all solvents investigated, $c_e > c_D$ and electrostatic interactions should not significantly perturb chain conformation.

By contrast, the apparent increase in $\eta_{sp}(c_e)$ with increasing ε suggests that the square of the number of binary interchain contacts required to form an entanglement increases with solvent permittivity. Since $\eta_{sp}(c_e)$ scales with the square of the number of contacts, this trend implies that the number of contacts required for entanglement formation is lower in low dielectric constant solvents. This behaviour could be rationalised by a reduced effective charge density at low ε, which would decrease the excluded volume between chains. However, if this interpretation were correct, a corresponding decrease in c_e with decreasing dielectric constant would also be expected.

Given the limited number of data points and the intrinsic difficulty of identifying entanglement transitions in polyelectrolyte solutions, we refrain from drawing firm conclusions.

D. Transition to associative rheology

In solvents such as water, ethylene glycol, and DMSO, TBACMC exhibits rheological behaviour similar to that of other hydrophilic polyelectrolytes, see fig. 1a-b, for example. By contrast, in alcohols a transition to associative solution rheology is observed. At sufficiently high concentrations, the flow curves do not display a Newtonian plateau at low shear rates, and the apparent viscosity increases with decreasing shear rate.

An additional example is shown in Fig. 8, which plots the apparent viscosity of TBACMC ($c = 0.02$ M) in six linear alcohols as a function of shear rate. The data are presented in an iso-friction representation, where the apparent viscosity is normalised by the solvent viscosity and the shear rate is multiplied by the solvent viscosity. In methanol and ethanol, the viscosity is largely Newtonian. For propanol, butanol, and pentanol, shear thinning becomes progressively more pronounced, consistent with increased interchain associations that lead to longer relaxation times.[25,26] In hexanol, the apparent viscosity decreases continuously with shear rate and no Newtonian plateau is observed.

The concentration at which the transition between Newtonian and shear-thinning behaviour in the low shear rate regime, denoted c_H, could not be determined with high precision. Instead, we identified one concentration at which a clear Newtonian plateau is present and another at which no Newtonian plateau is observed, and take the midpoint between these two concentrations as c_H. Figure 9 plots c_H for a series of linear alcohols and selected diols as a function of solvent di-

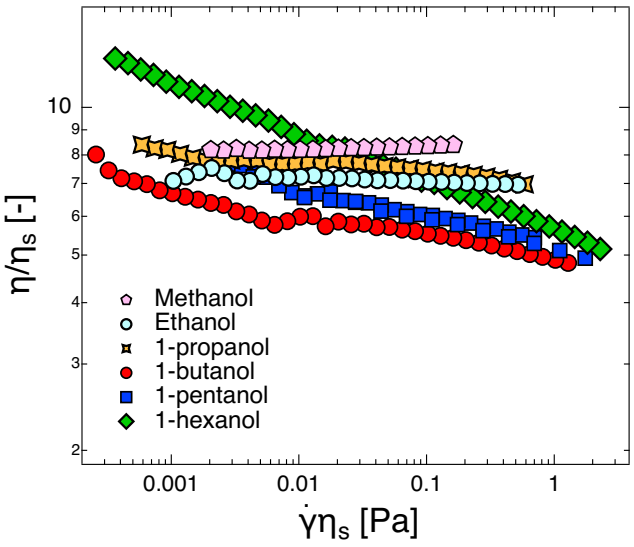

FIG. 8. Relative apparent viscosity vs. shear rate multiplied by solvent viscosity for $c = 0.0186$ M solutions of TBACMC in linear alcohols.

electric constant.

The data show that c_H decreases systematically with decreasing solvent permittivity. As the dielectric constant is lowered, the effective charge of the chain decreases, reducing the energetic penalty for interchain contacts. Stronger interchain associations then lead to longer relaxation times and more pronounced shear thinning. Dipole formation or charge–charge correlations may further enhance these associations.[16,17]

The behaviour observed here differs qualitatively from that reported for other associative polymer systems, including neutral polymers,[91] ionomers,[92] and polyelectrolytes.[25,93,94] It is also distinct from the behaviour of NaCMC in solvent–non-solvent mixtures, where decreasing solvent permittivity and solvent quality lead to gel formation rather than enhanced shear thinning.[43,45]

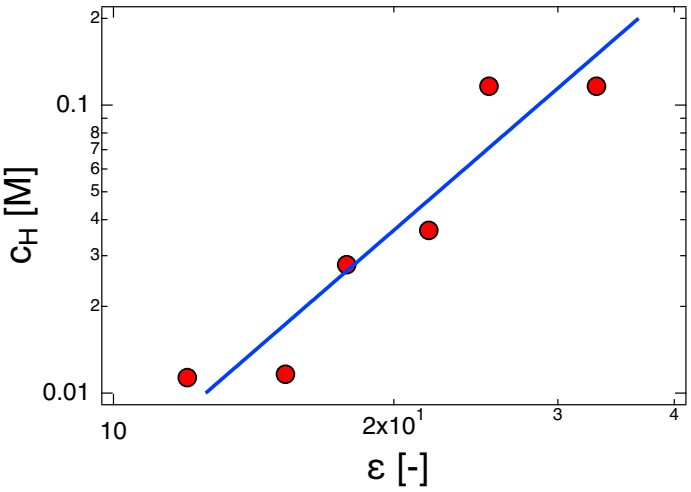

FIG. 9. Critical concentration at which solutions transition from Newtonian to shear thinning liquids in the low shear region, see for example figure 1c-d. Line is a guide to the eye.

Figure 10 compares the concentration dependence of the viscosity of TBACMC in four solvents. In water and ethylene glycol, no transition between non-associative and associative rheology is observed. The viscosity curves are parallel, with water exhibiting higher viscosities than EG, due to the higher charge fraction resulting in more extended chain conformations.

By contrast, in ethanol and methanol an associative transition occurs above $c \simeq 0.1$ M as discussed above. In these solvents, the viscosity is initially lower, consistent with more contracted chain conformations, but increases more rapidly as the concentration approaches the associative regime. This behaviour mirrors that observed for highly and weakly substituted CMC. While both display similar viscsosities in the non-entangled regime, weakly substituted CMC, which has stronger interchain associations, shows a much more rapid viscosity increase beyond the entanglement concentration, and eventually forms a physical gel.[26,36,95]

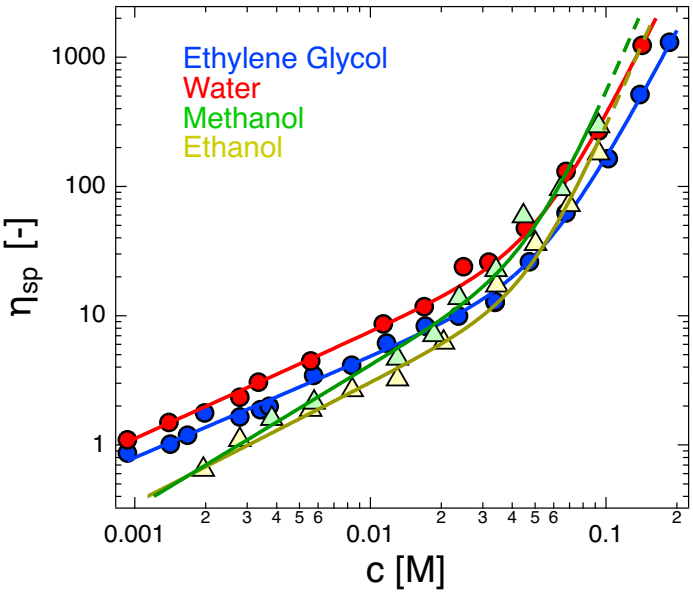

FIG. 10. Specific viscosity of TBACMC in non-associating solvents (ethylene glycol and water) and in associating solvents (methanol and ethanol). Lines are fits to Eq. 1.

E. Insight from SAXS

Figure 11 compares the scattering profiles of TBACMC solutions in the same set of linear alcohols shown in Fig. 8. In aqueous and other high-dielectric media, polyelectrolyte scattering is characterised by a correlation peak at intermediate q and an upturn at low q.[96–98] The correlation peak at $q = q^*$ reflects the suppression of concentration fluctuations on length-scales larger than the correlation length, $\xi = 2\pi/q^*$, due to the low osmotic compressibility of highly charged, salt-free polyelectrolyte solutions.[3,85,99,100] As the effective charge density decreases, the osmotic compressibility increases and the correlation peak is expected to weaken and eventually disappear

when fewer than one dissociated charges are present per correlation blob.[85]

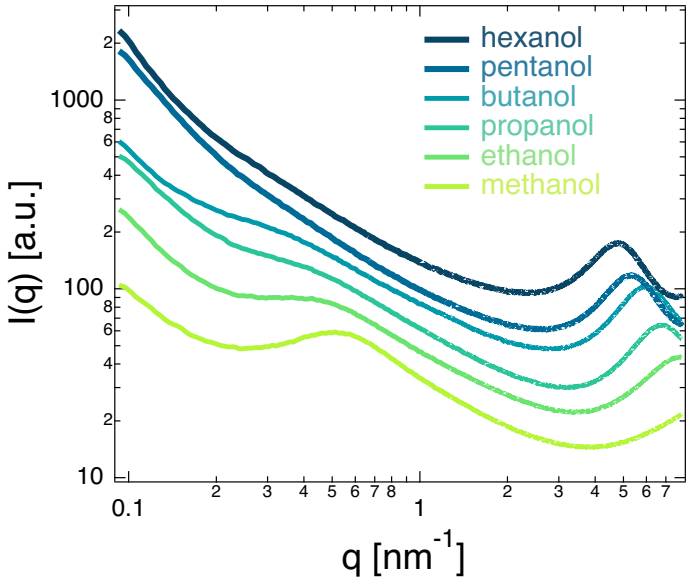

FIG. 11. SAXS intensities of c = 0.0307 M solutions of TBACMC in linear alcohols without added salts. Note the peak at high q, present for all samples, arises from the solvent. The intermediate q visible only for methanol and ethanol solution is a correlation peak, typical of polyelectrolytes in high permittivity solvents.

The interpretation of the low-q upturn is more controversial. The low osmotic compressibility of polyelectrolyte solutions should suppress long-wavelength density fluctuations, leading to weak scattering at low q.[101,102] For this reason, the low-q upturn has often been attributed to dust, undissolved polymer residues, or other impurities. The fact that the upturn can be reduced or removed by filtration[103–107] supports this interpretation, but the issue is still debated.[52,108–112] Independent of this, when polyelectrolytes are sufficiently weakly charged or sufficiently solvophobic, aggregation is expected to occur, which would enhance low-q scattering. Lowering the effective charge density both increases the osmotic compressibility and reduces the energetic penalty for interchain contacts, thereby facilitating aggregate formation.

The data in Fig. 11 are consistent with this picture. Methanol exhibits a clear correlation peak. In ethanol the peak is still present but less pronounced and shifted to lower q. This indicates an increase in the correlation length as the effective charge decreases. In propanol and butanol, the peak morphs into a shoulder, consistent with weaker suppression of concentration fluctuations and increased clustering, with the growing low-q contribution partially masking the peak. For pentanol and hexanol, the shoulder is barely discernible and the scattering is dominated by the low-q upturn, indicating stronger aggregation.

These scattering trends are in qualitative agreement with the interpretation of the rheological behaviour shown in Fig. 8, where increasingly pronounced shear thinning and the disappearance of a Newtonian plateau correlate with the onset of interchain associations which is also apparent from the SAXS data.

CONCLUSIONS

In salt-free solvents the overlap concentration decreases with increasing dielectric constant, with an approximately $c^* \propto \varepsilon^{-1}$ dependence, a weaker dependence than observed for flexible polyelectrolyte systems. In excess salt, the dielectric constant dependence is substantially weaker and at low dielectric permittivity, the salt-free and excess salt data display roughly the same overlap concentration, indicating that electrostatics perturb chains weakly. These trends are qualitatively consistent with increased counterion dissociation and stronger electrostatic chain expansion at higher permittivity, but quantitative comparison with scaling predictions is limited by the unknown solvent dependence of the Kuhn length.

In the semidilute regime, the unentangled viscosity exponent increases as the dielectric constant decreases, approaching the neutral polymer good-solvent value at low ε and remaining closer to polyelectrolyte-like behaviour at high ε. For sufficiently high concentrations but still below the entanglement point, the specific viscosity becomes independent of solvent permittivity, signalling that electrostatics do not influence chain conformation and dynamics, as expected for the 'neutral polymer' regime ($c > c_D$) predicted by the scaling theory at high polymer concentrations and/or low dielectric media.

The entanglement concentration shows no systematic dependence on dielectric constant over the solvents studied, consistent with entanglement occurring at concentrations above c_D where electrostatic interactions are strongly screened. In linear alcohols a distinct transition to associative rheology occurs at high concentrations. The critical concentration for the disappearance of the low-shear Newtonian plateau, c_H, decreases with decreasing dielectric constant, indicating that reduced effective charge promotes interchain associations and longer relaxation times. SAXS data in linear alcohols show a progressive weakening of the correlation peak and a strengthening of low-q scattering as dielectric constant decreases, consistent with the rheological signatures of increasing interchain association and aggregation in low-permittivity solvents.

ACKNOWLEDGEMENTS

We thank the SPring-8 synchrotron for beamtime (proposal numbers: 2024A1203, 2024A1606). This research was funded by the DFG grant: GO3250/2-1. We are grateful to Can Hou (RWTH), Atsushi Matsumoto (University of Fukui) and Takaichi Watanabe (University of Okayama) for help with the scattering experiments.

APPENDIX: SOLVENT PROPERTIES

BIBLIOGRAPHY

[1] A. V. Dobrynin and M. Rubinstein, "Theory of polyelectrolytes in solutions and at surfaces," Progress in polymer science **30**, 1049–1118 (2005).

Solvent	σ [μS/cm]	ρ [g/mL]	ε [-]	η [mPas]	δ_D [MPa$^{0.5}$]	δ_P [MPa$^{0.5}$]	δ_H [MPa$^{0.5}$]	Solution state
1-2 Dimethoxyethane	0.0161	0.8637	7.3	0.414	15.4	6.3	6	insoluble
1-Butanol (BuOH)	0.1795	0.8095	17.8	2.544	16	5.7	15.8	soluble
1-Decanol	-	0.8297	7.93	10.9	16	4.7	10	insoluble
1-Dodecanol	-	0.8309	5.82	18.8	16	4	9.3	insoluble
1-Hexanol (HexOH)	0.0062	0.8136 (0.8153)	13.03	4.578	15.9	5.8	12.5	soluble
1-Methyl-2-pyrrolidone	3.1275	1.027	32.2	1.65	18	12.3	7.2	insoluble
1-Octanol	-	0.8262	10.3	7.288	16	5	11.9	swollen/turbid
1-Pentanol (PeOH)	0.0289	0.8144 (0.8109)	15.13	3.619	15.9	5.9	13.9	soluble
1,2-Pentanediol	0.0962	0.9723	17.31	49.22				soluble
1-Propanol	0.1002	0.7997 (0.7996)	20.8	1.945	16	6.8	17.4	soluble
1,3-Propanediol	1.1525	1.0597	35	39.15	16.8	13.5	23.2	soluble
1,4 Dioxane	-	1.0337	2.22	1.177	19	1.8	7.4	insoluble
1,4-Butanediol	0.0331	1.0171	31.9	66.54	16.6	15.3	21.7	soluble
1.2-Butanediol	0.0208	1.0024	22.4	48.2				soluble
2-butanone	0.272	0.7999	18.56	0.405	16	9	5.1	insoluble
2-Ethyl-Hexanol	-	0.8319	7.58	6.271	15.9	3.3	11.8	insoluble
Acetone	0.301	0.7845	21.01	0.306	15.5	10.4	7	insoluble
Acetonitrile	0.1358	0.7857 (0.7767)	36.64	0.369	15.3	18	6.1	turbid
Benyzl Alcohol	0.2823	1.0419	11.92	5.474	18.4	6.3	13.7	insoluble
Benzaldehyde	2.2	1.0401	17.85	1.321	19.4	7.4	5.3	insoluble
Benzene	-	0.8765	2.28	0.604	18.4	0	2	insoluble
Chloroform	-	1.4788	4.81	0.537	17.8	3.1	5.7	insoluble
Dichloromethane	0.0285	1.3266	8.93	0.413	18.2	6.3	6.1	insoluble
Diethylene glycol	0.1123	1.1197	31.82	30.2	16.6	12	20.7	soluble
Dimethylsulfoxide	0.5437	1.101 (1.0956)	47.24	1.987	18.4	16.4	10.2	soluble
Dipropylene Glycol	-	1.0206	20	66.67	16.5	10.6	17.7	soluble
Epichlorohydrin	0.0275	1.1812	22.6	1.073	18.9	7.6	6.6	insoluble
Ethanol (EtOH)	0.1475	0.7893 (0.7856)	25.3	1.074	15.8	8.8	19.4	soluble
Ethyl Acetate	-	0.9003	6.08	0.423	15.8	5.3	7.2	insoluble
Ethylene Glycol (EG)	0.0836	1.1135 (1.1097)	41.4	16.1	17	11	26	soluble
Furfural	12.925	1.1594	42.1	1.587	18.6	14.9	5.1	insoluble
Hexane	-	0.6606	1.89	0.3	14.9	0	0	insoluble
IsoAmyl Alcohol	0.011	0.8104	15.63	3.692	15.8	5.2	13.3	soluble
IsobutylAlcohol	0.1728	0.8018	17.93	4	15.1	5.7	15.9	swollen/turbid
Isopropanol (IPA)	0.0247	0.7809	20.18	2.038	15.8	6.1	16.4	insoluble
Methanol (MeOH)	0.8225	0.7914 (0.7867)	33	0.544	15.1	12.3	22.3	soluble
Morpholine	0.0145	1.0005	7.42	2.021	18.8	4.9	9.2	insoluble
N-methyl Acetamide	10.5	0.9371	178.9	3.65	16.9	18.7	13.9	insoluble
N,N dimethylacrylamide	12.075	0.962						insoluble
N,N Dimethylformamide	1.1825	0.9445 (0.944)	38.25	0.794	17.4	13.7	11.3	soluble
Nitrobenzene	0.0148	1.2037	35.6	1.863	20	8.6	4.1	swollen/turbid
Pentanal	0.0353	0.8095	10	0.54	15.7	9.4	5.8	insoluble
Phenyl Ethyl Alcohol	0.0384	1.013	13	7.58	19	5.8	12.8	soluble
Propylene Carbonate	5.4175	1.2047	66.14	2.5009	20	18	4.1	swollen/turbid
Propylene Glycol	0.0057	1.0361	32	40.4	16.8	9.4	23.3	soluble
Pyridine	1.4525	0.9819	13.26	0.879	19	8.8	5.9	swollen/turbid
Tetrahydrofuran	0.0094	0.8833	7.52	0.456	16.8	5.7	8	insoluble
Toluene	-	0.8668	2.38	0.56	18	1.4	2	insoluble
Triethylene glycol	0.0457	1.1274	23.69	35.15	7.8	6.1	9.1	soluble
Tripropylene Glycol	0.0247	1.02	12	52.76				soluble
Water	2	0.997	80.1	0.89	15.5	16	42.3	soluble

TABLE III. Electrical conductivity of solvents used in this study (measured by us) and other parameters. Hansen solubility parameters taken from [113]. Densities and dielectric constants are from [114]. Density values in brackets are measured by us. The last column gives the solubility state of 1 wt% TBACMC.

[2] R. H. Colby, "Structure and linear viscoelasticity of flexible polymer solutions: comparison of polyelectrolyte and neutral polymer solutions," Rheologica acta **49**, 425–442 (2010).

[3] C. G. Lopez, A. Matsumoto, and A. Q. Shen, "Dilute polyelectrolyte solutions: recent progress and open questions," Soft Matter **20**, 2635–2687 (2024).

[4] F. Oosawa, "A simple theory of thermodynamic properties of polyelectrolyte solutions," Journal of Polymer Science **23**, 421–430 (1957).

[5] G. S. Manning, "Limiting laws and counterion condensation in polyelectrolyte solutions i. colligative properties," The journal of chemical Physics **51**, 924–933 (1969).

[6] F. Oosawa, *Polyelectrolytes* (MARCEL DEKKER, 1971).

[7] M. Beer, M. Schmidt, and M. Muthukumar, "The electrostatic expansion of linear polyelectrolytes: Effects of gegenions, co-ions, and hydrophobicity," Macromolecules **30**, 8375–8385 (1997).

[8] G. Chen, A. Perazzo, and H. A. Stone, "Electrostatics, conformation, and rheology of unentangled semidilute polyelectrolyte solutions," Journal of Rheology **65**, 507–526 (2021).

[9] A. Matsumoto, "Solution rheology of poly (ionic liquid) s: current understanding and open questions," Korea-Australia Rheology Journal **36**, 319–328 (2024).

[10] A. Matsumoto, "Rheology of polyelectrolyte solutions: current understanding and perspectives," Nihon Reoroji Gakkaishi **50**, 43–50 (2022).

[11] A. Matsumoto, R. Ukai, H. Osada, S. Sugihara, and Y. Maeda, "Tuning the solution viscosity of ionic-liquid-based polyelectrolytes with solvent dielectric constants via the counterion condensation," Macromolecules **55**, 10600–10606 (2022).

[12] H. Schiessel and P. Pincus, "Counterion-condensation-induced collapse of highly charged polyelectrolytes," Macromolecules **31**, 7953–7959 (1998).

[13] H. Schiessel, "Counterion condensation on flexible polyelectrolytes: Dependence on ionic strength and chain concentration," Macromolecules **32**, 5673–5680 (1999).

[14] M. Muthukumar, "Theory of counter-ion condensation on flexible polyelectrolytes: Adsorption mechanism," The Journal of chemical physics **120**, 9343–9350 (2004).

[15] Q. Liao, A. V. Dobrynin, and M. Rubinstein, "Counterion-correlation-induced attraction and necklace formation in polyelectrolyte solutions: Theory and simulations," Macromolecules **39**, 1920–1938 (2006).

[16] A. Cherstvy, "Collapse of highly charged polyelectrolytes triggered by attractive dipole- dipole and correlation-induced electrostatic interactions,"

The Journal of Physical Chemistry B **114**, 5241–5249 (2010).
[17] A. Gulati, L. Meng, T. Watanabe, and C. G. Lopez, "Electrostatically-driven collapse of polyelectrolytes: The role of the solvent's dielectric constant," Journal of Polymer Science **63** (2025).
[18] A. Gulati, L. Meng, T. Hou, Can Watanabe, and C. G. Lopez, "Solution structure and counterion condensation of carboxymethyl cellulose in organic solvents," (2025).
[19] A. V. Dobrynin, R. Sayko, and R. H. Colby, "Viscosity of polymer solutions and molecular weight characterization," ACS Macro Letters **12**, 773–779 (2023).
[20] S. Dou and R. H. Colby, "Solution rheology of a strongly charged polyelectrolyte in good solvent," Macromolecules **41**, 6505–6510 (2008).
[21] S. Dou and R. H. Colby, "Charge density effects in salt-free polyelectrolyte solution rheology," Journal of Polymer Science Part B: Polymer Physics **44**, 2001–2013 (2006).
[22] C. G. Lopez, "Entanglement properties of polyelectrolytes in salt-free and excess-salt solutions," ACS Macro Letters **8**, 979–983 (2019).
[23] A. Gulati, M. Jacobs, C. G. Lopez, and A. V. Dobrynin, "Salt effect on the viscosity of semidilute polyelectrolyte solutions: sodium polystyrenesulfonate," Macromolecules **56**, 2183–2193 (2023).
[24] D. Szopinski, W.-M. Kulicke, and G. A. Luinstra, "Structure–property relationships of carboxymethyl hydroxypropyl guar gum in water and a hyperentanglement parameter," Carbohydrate polymers **119**, 159–166 (2015).
[25] M. Ganesan, S. Knier, J. G. Younger, and M. J. Solomon, "Associative and entanglement contributions to the solution rheology of a bacterial polysaccharide," Macromolecules **49**, 8313–8321 (2016).
[26] C. G. Lopez, R. H. Colby, and J. T. Cabral, "Electrostatic and hydrophobic interactions in nacmc aqueous solutions: Effect of degree of substitution," Macromolecules **51**, 3165–3175 (2018).
[27] C. Hoogendam, A. De Keizer, M. Cohen Stuart, B. Bijsterbosch, J. Smit, J. Van Dijk, P. Van Der Horst, and J. Batelaan, "Persistence length of carboxymethyl cellulose as evaluated from size exclusion chromatography and potentiometric titrations," Macromolecules **31**, 6297–6309 (1998).
[28] C. G. Lopez, "Entanglement of semiflexible polyelectrolytes: Crossover concentrations and entanglement density of sodium carboxymethyl cellulose," Journal of Rheology **64**, 191–204 (2020).
[29] A. G. et al, "The electrostatic expansion of linear polyelectrolytes: Effects of gegenions, co-ions, and hydrophobicity," Cellulose, submitted.
[30] V. Stigsson, G. Kloow, and U. Germgård, "An historic overview of carboxymethyl cellulose (cmc) production on an industrial scale," PaperAsia **17** (2001).
[31] E. Debutts, J. Hudy, and J. Elliott, "Rheology of sodium carboxymethylcellulose solutions," Industrial & Engineering Chemistry **49**, 94–98 (1957).
[32] P. S. Francis, "Solution properties of water-soluble polymers. i. control of aggregation of sodium carboxymethylcellulose (cmc) by choice of solvent and/or electrolyte," Journal of Applied Polymer Science **5**, 261–270 (1961).
[33] J. Elliott and A. Ganz, "Modification of food characteristics with cellulose hydrocolloids i: Rheological characterization of an organoleptic property (unctuousness)," Journal of Texture Studies **2**, 220–229 (1971).
[34] J. H. Elliot and A. Ganz, "Some rheological properties of sodium carboxymethylcellulose solutions and gels," Rheologica Acta **13**, 670–674 (1974).
[35] C. Barba, D. Montané, X. Farriol, J. Desbrières, and M. Rinaudo, "Synthesis and characterization of carboxymethylcelluloses from non-wood pulps ii. rheological behavior of cmc in aqueous solution," Cellulose **9**, 327–335 (2002).
[36] C. G. Lopez and W. Richtering, "Oscillatory rheology of carboxymethyl cellulose gels: Influence of concentration and ph," Carbohydrate polymers **267**, 118117 (2021).
[37] C. G. Lopez, S. E. Rogers, R. H. Colby, P. Graham, and J. T. Cabral, "Structure of sodium carboxymethyl cellulose aqueous solutions: A sans and rheology study," Journal of Polymer Science Part B: Polymer Physics **53**, 492–501 (2015).
[38] M. Yoshida, D. Nakagawa, H. Hozumi, Y. Horikawa, S. Makino, H. Nakamura, and T. Shikata, "A new concept for interpretation of the viscoelastic behavior of aqueous sodium carboxymethyl cellulose systems," Biomacromolecules **25**, 3420–3431 (2024).
[39] C. Hou, T. Watanabe, C. G. Lopez, and W. Richtering, "Structure and rheology of carboxymethylcellulose in polar solvent mixtures," Carbohydrate Polymers **347**, 122287 (2025).
[40] P. Nandi and B. Das, "Effects of concentration, relative permittivity, and temperature on the solution behavior of sodium carboxymethylcellulose as probed by electrical conductivity," The Journal of Physical Chemistry B **109**, 3238–3242 (2005).
[41] A. Chatterjee, B. Das, and C. Das, "Polyion–counterion interaction behavior for sodium carboxymethylcellulose in methanol–water mixed solvent media," Carbohydrate polymers **87**, 1144–1152 (2012).
[42] L. N. Jimenez, C. D. Martinez Narvaez, and V. Sharma, "Solvent properties influence the rheology and pinching dynamics of polyelectrolyte solutions thickening the pot with glycerol and cellulose gum," Macromolecules **55**, 8117–8132 (2022).
[43] P. Wagner, S. Różańska, E. Warmbier, A. Frankiewicz, and J. Różański, "Rheological properties of sodium carboxymethylcellulose solutions in dihydroxy alcohol/water mixtures," Materials **16**, 418 (2023).
[44] S. Różańska, K. Verbeke, J. Różański, C. Clasen, and P. Wagner, "Capillary breakup extensional rheometry of sodium carboxymethylcellulose solutions in water and propylene glycol/water mixtures," Journal of Polymer Science Part B: Polymer Physics **57**, 1537–1547 (2019).
[45] P. Komorowska, S. Różańska, and J. Różański, "Effect of the degree of substitution on the rheology of sodium carboxymethylcellulose solutions in propylene glycol/water mixtures," Cellulose **24**, 4151–4162 (2017).
[46] G. Legrand, G. P. Baeza, M. Peyla, L. Porcar, C. Fernandez-de Alba, S. Manneville, and T. Divoux, "Acid-induced gelation of carboxymethylcellulose solutions," ACS Macro Letters **13**, 234–239 (2024).
[47] G. Legrand, G. P. Baeza, S. Manneville, and T. Divoux, "Rheological properties of acid-induced carboxymethylcellulose hydrogels," Cellulose , 1–15 (2024).
[48] R. Barbucci, A. Magnani, and M. Consumi, "Swelling behavior of carboxymethylcellulose hydrogels in relation to cross-linking, ph, and charge density," Macromolecules **33**, 7475–7480 (2000).
[49] A. Gulati and C. G. Lopez, "Viscosity of polyelectrolytes: Influence of counterion and solvent type," ACS Macro Letters **13**, 1079–1083 (2024).
[50] C. Hou, W. Richtering, T. Watanabe, K. Leonhard, M. Papusha, and C. G. Lopez, "Solutions of carboxymethylcellulose with organic counterions (i): The influence of counterion properties on the polymer structure and solubility," Macromolecules (2025).
[51] H. Vink, "Studies of electrical transport processes in polyelectrolyte solutions," Journal of the Chemical Society, Faraday Transactions 1: Physical Chemistry in Condensed Phases **85**, 699–709 (1989).
[52] A. Gulati, J. F. Douglas, O. Matsarskaia, and C. G. Lopez, "Influence of counterion type on the scattering of a semiflexible polyelectrolyte," Soft matter **20**, 8610–8620 (2024).
[53] C. Hou, T. Watanabe, W. Richtering, K. Leonhard, M. Papusha, and C. G. Lopez, "Solutions of carboxymethylcellulose with organic counterions (ii): the effect of solvent quality and dielectric constant on counterion dissociation," In preparation.
[54] C. G. Lopez, R. H. Colby, P. Graham, and J. T. Cabral, "Viscosity and scaling of semiflexible polyelectrolyte nacmc in aqueous salt solutions," Macromolecules **50**, 332–338 (2017).
[55] M. K. Kwon, J. Lee, K. S. Cho, S. J. Lee, H. C. Kim, S. W. Jeong, and S. G. Lee, "Scaling analysis on the linear viscoelasticity of cellulose 1-ethyl-3-methyl imidazolium acetate solutions," Korea-Australia Rheology Journal **31**, 123–139 (2019).
[56] S. Jousset, H. Bellissent, and J. C. Galin, "Polyelectrolytes of high charge density in organic solvents. synthesis and viscosimetric behavior," Macromolecules **31**, 4520–4530 (1998).
[57] M. Muthukumar, *Physics of Charged Macromolecules* (Cambridge University Press, 2023).
[58] D. C. Boris and R. H. Colby, "Rheology of sulfonated polystyrene solutions," Macromolecules **31**, 5746–5755 (1998).
[59] C. G. Lopez, "Scaling and entanglement properties of neutral and sulfonated polystyrene," Macromolecules **52**, 9409–9415 (2019).
[60] M. Muthukumar, "Double screening in polyelectrolyte solutions: Limiting laws and crossover formulas," The Journal of chemical physics **105**, 5183–5199 (1996).
[61] Note that while the theory of Muthukumar does not expect the Oosawa-Manning condensation to hold except for rigid-rod polyelectrolytes, exper-

imentally, we observe that $f \propto l_B^{-1}$ for TBACMC in the solvents studied here.
[62] J. W. Mays, N. Hadjichristidis, and L. J. Fetters, "Solvent and temperature influences on polystyrene unperturbed dimensions," Macromolecules **18**, 2231–2236 (1985).
[63] L. J. Fetters, N. Hadjichristidis, J. Lindner, J. Mays, and W. Wilson, "Transport properties of polyisobutylene in dilute solution," Macromolecules **24**, 3127–3135 (1991).
[64] A. Boothroyd, A. Rennie, and G. Wignall, "Temperature coefficients for the chain dimensions of polystyrene and polymethylmethacrylate," The Journal of chemical physics **99**, 9135–9144 (1993).
[65] K. Horita, F. Abe, Y. Einaga, and H. Yamakawa, "Excluded-volume effects on the intrinsic viscosity of oligo-and polystyrenes. solvent effects," Macromolecules **26**, 5067–5072 (1993).
[66] S. Dayan, P. Maissa, M. Vellutini, and P. Sixou, "Intrinsic viscosity of cellulose derivatives and the persistent cylinder model of yamakawa," Polymer **23**, 800–804 (1982).
[67] K. Kamide and M. Saito, "Cellulose and cellulose derivatives: Recent advances in physical chemistry," Biopolymers , 1–56 (2005).
[68] K. Kamide, T. Terakawa, and Y. Miyazaki, "The viscometric and light-scattering determination of dilute solution properties of cellulose diacetate," Polymer Journal **11**, 285–298 (1979).
[69] K. Kamide, M. Saito, and H. Suzuki, "Persistence length of cellulose and cellulose derivatives in solution," Die Makromolekulare Chemie, Rapid Communications **4**, 33–39 (1983).
[70] K. Kamide, Y. Miyazaki, and T. Abe, "Dilute solution properties and unperturbed chain dimension of cellulose triacetate," Polymer Journal **11**, 523–538 (1979).
[71] L. Schulz, B. Seger, and W. Burchard, "Structures of cellulose in solution," Macromolecular chemistry and physics **201**, 2008–2022 (2000).
[72] W. Burchard, "Solubility and solution structure of cellulose derivatives," Cellulose **10**, 213–225 (2003).
[73] A. Gupta, J. Cotton, E. Marchal, W. Burchard, and H. Benoit, "Persistence length of cellulose tricarbanilate by small-angle neutron scattering," Polymer **17**, 363–366 (1976).
[74] K. Kamide, M. Saito, and T. Abe, "Dilute solution properties of water-soluble incompletely substituted cellulose acetate," Polymer Journal **13**, 421–431 (1981).
[75] C. G. Lopez, A. Matsumoto, A. Gulati, C. Hou, Y. Mizutani, H. Osada, Y. Tao, K. Fujii, W. Richtering, and T. Watanabe, "Structure of poly (ionic liquid) s in solutions: a small angle scattering study," (2023).
[76] A. Han and R. H. Colby, "Rheology of entangled polyelectrolyte solutions," Macromolecules **54**, 1375–1387 (2021).
[77] Although the chain size exhibits the same dependence on dielectric constant in the salt-free and excess-salt limits, the underlying physical mechanisms differ.
[78] M. Muthukumar, "50th anniversary perspective: A perspective on polyelectrolyte solutions," Macromolecules **50**, 9528–9560 (2017).
[79] P. J. Flory, "Molecular configuration of polyelectrolytes," The Journal of Chemical Physics **21**, 162–163 (1953).
[80] J. S. Behra, J. Mattsson, O. J. Cayre, E. S. Robles, H. Tang, and T. N. Hunter, "Characterization of sodium carboxymethyl cellulose aqueous solutions to support complex product formulation: A rheology and light scattering study," ACS Applied Polymer Materials **1**, 344–358 (2019).
[81] C. G. Lopez and W. Richtering, "Viscosity of semidilute and concentrated nonentangled flexible polyelectrolytes in salt-free solution," The Journal of Physical Chemistry B **123**, 5626–5634 (2019).
[82] A. Han, V. V. S. Uppala, D. Parisi, C. George, B. J. Dixon, C. D. Ayala, X. Li, L. A. Madsen, and R. H. Colby, "Determining the molecular weight of polyelectrolytes using the rouse scaling theory for salt-free semidilute unentangled solutions," Macromolecules **55**, 7148–7160 (2022).
[83] A. V. Dobrynin and M. Jacobs, "When do polyelectrolytes entangle?" Macromolecules **54**, 1859–1869 (2021).
[84] M. Rubinstein and R. H. Colby, *Polymer physics* (Oxford university press, 2003).
[85] A. V. Dobrynin, R. H. Colby, and M. Rubinstein, "Scaling theory of polyelectrolyte solutions," Macromolecules **28**, 1859–1871 (1995).
[86] M. Jacobs, C. G. Lopez, and A. V. Dobrynin, "Quantifying the effect of multivalent ions in polyelectrolyte solutions," Macromolecules **54**, 9577–9586 (2021).
[87] C. G. Lopez, J. Linders, C. Mayer, and W. Richtering, "Diffusion and viscosity of unentangled polyelectrolytes," Macromolecules **54**, 8088–8103 (2021).
[88] A. Matsumoto, C. Zhang, F. Scheffold, and A. Q. Shen, "Microrheological approach for probing the entanglement properties of polyelectrolyte solutions," ACS Macro Letters **11**, 84–90 (2021).
[89] A. Matsumoto, I. Kato, C. Zhang, S. Sugihara, Y. Maeda, F. Scheffold, and A. Q. Shen, "Microrheological study on the entanglement dynamics of salt-free polyelectrolyte solutions in the semidilute entangled regime," Polymer Journal **57**, 1215–1225 (2025).
[90] Y. Rharbi, "Scaling behavior of entanglement dynamics in polyelectrolyte solutions: Insights from high-frequency rheometry," ACS Macro Letters **14**, 259–264 (2025).
[91] D. Parisi, C. D. Ditillo, A. Han, S. Lindberg, M. W. Hamersky, and R. H. Colby, "Rheological investigation on the associative properties of poly (vinyl alcohol) solutions," Journal of Rheology **66**, 1141–1150 (2022).
[92] D. Peiffer, J. Kaladas, I. Duvdevani, and J. Higgins, "Time-and shear-rate-dependent rheology of ionomer solutions," Macromolecules **20**, 1397–1400 (1987).
[93] P. Kujawa, A. Audibert-Hayet, J. Selb, and F. Candau, "Effect of ionic strength on the rheological properties of multisticker associative polyelectrolytes," Macromolecules **39**, 384–392 (2006).
[94] P. Kujawa, A. Audibert-Hayet, J. Selb, and F. Candau, "Rheological properties of multisticker associative polyelectrolytes in semidilute aqueous solutions," Journal of Polymer Science Part B: Polymer Physics **42**, 1640–1655 (2004).
[95] U. Kastner, H. Hoffmann, R. Do, J. Hilbig, *et al.*, "Structure and solution properties of sodium carboxymethyl cellulose," Colloids and Surfaces A: Physicochemical and Engineering Aspects **123**, 307–328 (1997).
[96] F. Horkay and B. Hammouda, "Small-angle neutron scattering from typical synthetic and biopolymer solutions," Colloid and Polymer Science **286**, 611–620 (2008).
[97] B. Hammouda, F. Horkay, and M. L. Becker, "Clustering and solvation in poly (acrylic acid) polyelectrolyte solutions," Macromolecules **38**, 2019–2021 (2005).
[98] B. Hammouda, "Clustering in polar media," The Journal of chemical physics **133** (2010).
[99] P.-G. De Gennes, P. Pincus, R. Velasco, and F. Brochard, "Remarks on polyelectrolyte conformation," Journal de physique **37**, 1461–1473 (1976).
[100] G. Weill, "Conformation and order in polyelectrolyte solutions," Journal de Physique **49**, 1049–1054 (1988).
[101] Z. Alexandrowicz, "The correlation between activities of polyelectrolytes, measured by the light-scattering and osmotic methods," Journal of Polymer Science **40**, 91–106 (1959).
[102] A. Katchalsky, "Polyelectrolytes and their biological interactions," Biophysical journal **4**, 9–41 (1964).
[103] S. Ghosh, R. M. Peitzsch, and W. F. Reed, "Aggregates and other particles as the origin of the "extraordinary" diffusional phase in polyelectrolyte solutions," Biopolymers: Original Research on Biomolecules **32**, 1105–1122 (1992).
[104] R. C. Michel and W. F. Reed, "New evidence of the nonequilibrium nature of the "slow modes" of diffusion in polyelectrolyte solutions," Biopolymers: Original Research on Biomolecules **53**, 19–39 (2000).
[105] E. Josef and H. Bianco-Peled, "Conformation of a natural polyelectrolyte in semidilute solutions with no added salt," Soft Matter **8**, 9156–9165 (2012).
[106] M. Spiteri, "Conformation and arrangement of polyelectrolytes in semidiluted solution. a study by small angle neutrons scattering; conformation et arrangement des polyelectrolytes en solution semi-diluee. etude par diffusion des neutrons aux petits angles," (1997).
[107] A. Gulati, *Polyelectrolyte conformation and rheology in solutions*, Ph.D. thesis, Dissertation, RWTH Aachen University, 2024 (2024).
[108] B. Hammouda, "The mystery of clustering in macromolecular media," Polymer **50**, 5293–5297 (2009).
[109] W. Essafi, A. Abdelli, G. Bouajila, and F. Boué, "Behavior of hydrophobic polyelectrolyte solution in mixed aqueous/organic solvents revealed by neutron scattering and viscosimetry," The Journal of Physical Chemistry B **116**, 13525–13537 (2012).
[110] W. Essafi, W. Raissi, A. Abdelli, and F. Boué, "Metastability of large aggregates and viscosity, and stability of the pearl necklace conformation

after organic solvent treatment of aqueous hydrophobic polyelectrolyte solutions," The Journal of Physical Chemistry B **118**, 12271–12281 (2014).
[111]J. F. Douglas, F. Horkay, and Y. Zhang, "Influence of counterion valency on the scattering properties of highly charged polyelectrolyte solutions revisited," The Journal of Chemical Physics **163** (2025).
[112]M. Sedlak, "Resolving the mystery of the extraordinary polyelectrolyte behavior (anomalously slow diffusive mode) after half-century of research," Macromolecules **58**, 5329–5343 (2025).
[113]C. M. Hansen, *Hansen solubility parameters: a user's handbook* (CRC press, 2007).
[114]D. Lide, "Crc handbook of chemistry and physics, vol. 85, 2004,".